Simulation of Semi-Crystalline Composites in the Extrusion Deposition Additive Manufacturing Process

Bastian Brenken, Eduardo Barocio, Anthony J. Favaloro and R. Byron Pipes

Purdue University

Composites Manufacturing & Simulation Center

1105 Challenger Avenue, Suite 100

West Lafayette, IN, 47906

Abstract: *A UMATHT user subroutine was developed in Abaqus to combine a non-isothermal dual crystallization kinetics model with a statistical melting model in order to describe the simultaneous solidification/re-melting behavior of 3D printed parts during the Extrusion Deposition (ED) process. This subroutine is described in detail. Results indicate that crystallization behavior is significant and strongly dependent on the utilized polymer. As an outlook, the interaction with a second UMAT user subroutine that will be employed to predict residual stresses and deformations is explained.*

Recent developments in additive manufacturing have been made in ED. In order to improve stiffness and minimize warpage of printed parts, polymers with fiber reinforcement have gained special interest. Tools and molds are a promising application for this technology. In order to print carbon-fiber composite tooling, a high thermal stability of the printed tool is essential to maintain shape throughout multiple thermal cycles. Consequently, high temperature thermoplastics with high fiber contents should be employed. Semi-crystalline polymers like polyphenylene sulfide (PPS) or polyether ether ketone (PEEK) are potential candidates. Their partially crystalline structure adds significant thermal stability, but also additional shrinkage during cool down. Therefore, a crystallization simulation needs to be included in an overall solidification analysis to predict the residual stress and deformation state of printed tools.

The presented work with focus on the modeling of material crystallization is believed to be an essential step towards a complete solidification simulation of 3D printed carbon fiber tooling and parts.

1. Introduction

1.1 Extrusion Deposition Process

Extrusion Deposition (ED) is an Additive Manufacturing (AM) technique that has evolved significantly during the last five years. It is also known as Fused Filament Fabrication (FFF) or Fused Deposition Modeling (FDM). In contrast to classical subtractive methods, the ED method enables to build a part in a layer wise deposition process of molten material. This material is extruded in the form of circular beads to form the final part.

Major technical advancements have been achieved in recent years. In a collaboration with Cincinnati Incorporated, the Oakridge National Laboratory developed the Big Area Additive Manufacturing (BAAM) printer, a large scale ED printer (Oarkridge National Laboratory, 2016). Large objects like cars and even a small house were successfully printed with this machine (Sawyer, 2016). However, the current main application of large scale ED is tooling due to reduced strength requirements. With this target application of tooling, the company Thermwood developed a large scale ED printer as well, the Large Scale Additive Manufacturing (LSAM) system (Thermwood, 2016). The extension to the large scale is possible by the addition of carbon fibers to the printing material. These fibers significantly lower the resulting warpage of printed parts and enhance the mechanical properties (Love, et al., 2014). Furthermore, the fibers reduce the coefficient of thermal expansion of the printed material in the printing direction, which offers the potential to control and design the expansion behavior of printed tools.

1.2 Polymer Crystallization

While traditional printing materials like Polyactic acid (PLA) and Acrylonitrile Butadiene Styrene (ABS) are amorphous, printable semi-crystalline polymers exist as well. In order to print high temperature tooling for autoclave and compression molding applications, Polyphenylene Sulfide (PPS) is a potential candidate. It is a high temperature engineering polymer and material testing at Purdue University has confirmed it's applicability to autoclave conditions. Compared to the amorphous polymer PEI with similar properties, it is about 60% less expensive (DeNardo, 2016), which makes it the preferred choice. However, PPS is a semi-crystalline polymer, which induces additional complexity to the simulation of the printing process. Semi-crystalline polymers crystallize when cooling down from the melt. The crystallization kinetics are governed by nucleation and growth. While the nucleation describes the formation of a polymer crystal, the growth defines its increase in size. Polymer crystallization is an exothermic process. This means that heat is released during the phase change and the crystallization reaction is strongly coupled with the heat transfer analysis. However, in this paper, the enthalpy of crystallization was not considered since for thermoplastic polymers, it is usually an order of magnitude lower than the heat capacity of the material (Chapman, Gillespie, Pipes, Manson, & Seferis, 1990).

During the crystallization process, the mechanical and thermal properties change. Furthermore, polymer crystallization induces additional shrinkage to the material, and for accurate predictions of the part deformations during printing, this additional shrinkage has to be captured. For these reasons, a prediction of the evolution of crystallinity is essential for a realistic printing simulation of semi-crystalline polymers. This paper illustrates how Abaqus can be utilized with a custom UMATHT user subroutine to model the evolution of crystallinity during an ED printing process.

1.3 Additive Manufacturing Simulation Capabilities in Abaqus 2017

In the latest release of Abaqus 2017, a powerful new tool was implemented that allows for the realistic molding of the ED printing process. The machine code that controls the movement of the printer during the actual printing process can be implemented as an event series in Abaqus. It is a table consisting of the time and x,y,z data of the printing head during the deposition process. With the aid of this event series, the ED process can be simulated. First, a part-unspecific mesh is required. At the beginning of an analysis, the elements of this mesh are inactive. The new Abaqus user subroutine UEPActivationVol can then be utilized to activate elements for the analysis. The time and x,y,z information from the event series as well as information about the geometry of the extruded bead cross sections are employed for this activation routine. Since the activation is performed based on the actual machine code used for printing, the real printing process can be modeled accurately (Dassault Systémes Simulia Corp., 2017).

Fiber-reinforced polymers are anisotropic materials that have a direction dependence of mechanical and thermal properties. During the printing process, most of the fibers align parallel to the printing direction (Heller, Smith, & Jack, 2016). Therefore, orientations need to be assigned to the activated elements in order to allow for an accurate physics simulation. Here, the user subroutine ORIENT can be used. It is possible to define material orientations based on the local orientation of the extruded beads, which can be computed from the event series information (Dassault Systémes Simulia Corp., 2017). More detailed information about the simulation of the printing process and the orientation definitions can be found in the paper by Favaloro et al. (Favaloro, Brenken, Barocio, & Pipes, 2017).

2. Material Models

In this section, the utilized phenomenological models to describe the crystallization kinetics and melting behavior are introduced. These models were chosen based on experimental data and then fitted to the experimental results in order to describe the crystallization and re-melting behavior of the material.

2.1 Crystallization Kinetics

The dual crystallization kinetics model by Velisaris and Seferis (Velisaris & Seferis, 1986) was developed to describe the non-isothermal crystallization behavior of a fiber-reinforced high temperature polymer. It is able to capture and describe two crystallization mechanisms that are occurring at the same time. For fiber-reinforced polymers, the fibers affect the crystallization behavior. Often, the fibers act as nucleation sites for crystals, which is called heterogeneous crystallization. Here, the resulting crystals have a different shape as those which nucleated in the bulk material (homogeneous nucleation). A dual model is able to account for these two mechanisms. The model expresses the volume crystallinity X_{vc} as (Velisaris & Seferis, 1986):

$$X_{vc} = X_{vc\infty}(w_1 F_{vc1} + w_2 F_{vc2}) \tag{1}$$

Here, F_{vc1} and F_{vc2} represent a crystallization process each, while w_1 and w_2 express their relative importance ($w_1 + w_2 = 1$). $X_{vc\infty}$ describes the maximum volume crystallinity. Each of the crystallization processes is defined by (Velisaris & Seferis, 1986):

$$F_{vc,i} = 1 - exp\left[-C_{i1}\int_0^t T \cdot exp\left\{\frac{-C_{i2}}{T-T_g+T_{add,i}} - \frac{C_{i3}}{T(T_{m,i}-T)^2}\right\} n_i t^{n_i-1} dt\right], i = 1,2 \qquad (2)$$

This expression is both time and temperature independent. The non-isothermal nature of this equation is implemented by the integrals describing a time summation of an infinite number of isothermal segments between t and $t + dt$. The Avrami exponents n_i, $i = 1,2$ have to be determined in isothermal crystallization experiments (Velisaris & Seferis, 1986). They have no clear physical interpretation, but vary based on the dimension of crystal growth and the nucleation behavior. The exponents of the exponential in the integrand expression drive the evolution of crystallinity. The second C_{i3}-term describes the free enthalpy of nucleation. As soon as the material starts to cool down and the temperature starts to deviate more and more from the crystal melting temperature $T_{m,i}$ of the corresponding process, the term becomes more and more significant and the crystallization starts. When the temperature approaches the glass transition temperature T_g on the lower range of temperatures, the first C_{i2}-term increases and stops the crystallization process. $T_{add,i}$ is a parameter to provide adaptability in the fitting process. This first term describes the temperature dependence of viscosity and represents an increasing viscosity which becomes too large at low temperatures to let further crystallization take place. More details one the specific parts of Equation (2) can be found here (Wunderlich, 1976).

The presented model was developed for fiber-reinforced PEEK material (Velisaris & Seferis, 1986). However, it was also applied to predict the crystallinity of fiber-reinforced PPS already (Desio & Rebenfeld, 1992). Therefore, it is assumed to be a suitable model for describing the crystallization kinetics of high temperature composite materials for the ED process in general, which is why it was chosen for implementation in Abaqus.

2.2 Melting behavior

When hot, molten material is deposited onto previously laid down material during the ED process, the hot material wets and re-melts adjacent, already cooled down beads. In order to describe this re-melting process, a melting model is required. For this study, a statistical melting model was chosen. It was developed assuming a statistical distribution of crystal sizes in the material that evolve during polymer crystallization. Based on this assumption, the model relates a corresponding range of melting temperatures to the crystal size distribution presuming that a large crystal needs a higher temperature for re-melting. Statistical models are able to describe the melting material of semi-crystalline materials accurately as long as no rate dependent effects are dominant during the re-melting process. Then, a kinetics model is required (Greco & Maffezzoli, 2003).

For the current simulations, the following statistical, temperature dependent melting model is proposed (Greco & Maffezzoli, 2003):

$$\frac{dX_m}{dT}(T) = k_{mb}\{exp[-k_{mb}(T - T_c)]\} \cdot (1 + (d - 1)\exp[-k_{mb}(T - T_c)])^{\frac{d}{1-d}} \qquad (3)$$

The degree of melting X_m is assumed to be governed by a sigmoidal growth curve. In the model, T_c is the peak melting temperature corresponding to the maximum of the endothermic peak in the DSC experiment, k_{mb} is an intensity factor related to the sharpness of the distribution and d is a shape factor controlling the dispersion of melting temperatures lower than T_c. Outside the relevant range of melting temperatures, the model sets the degree of melting to zero at lower temperatures

and to one at higher temperatures. Thus a zero value corresponds to a solid material, while $X_m = 1$ means that the material is fully molten.

The degree of melting can be related to the volume crystallinity X_{vc} by assuming that for a fully molten material, the crystallinity X_{vc} equals zero. More details on the implementation of the combined melting/crystallization material behavior are provided in the next section.

3. Implementation in Abaqus

For the implementation of the presented material models in Abaqus, incremental versions of the models are needed. With these incremental forms, a UMATHT user subroutine can be employed to define the material behavior in Abaqus. When examining Equation (2), it becomes apparent that the integrals $I_i, i = 1,2$ can be defined as

$$\frac{\partial I_i}{\partial t} = C_{i1} T exp\left\{\frac{-C_{i2}}{T-T_g+T_{add,i}} - \frac{C_{i3}}{T(T_{m,i}-T)^2}\right\} n_i t^{n_i-1}, \ i = 1,2 \tag{4}$$

The incremental integral contribution of a certain time step can then be estimated using the mid-point approximation

$$\Delta I_i \approx C_{i1} T_m exp\left\{\frac{-C_{i2}}{T_m-T_g+T_{add,i}} - \frac{C_{i3}}{T_m(T_{m,i}-T_m)^2}\right\} n_i t_m^{n_i-1}\Delta t, \ i = 1,2 \tag{5}$$

Here, t_m is the mid time of the time interval, T_m the mid interval temperature and Δt the interval length. However, the time has to be corrected with the activation time t_{act} of the material during the analysis. This is described in more detail below. The evolution of crystallinity is then defined by the sum of all contributions ΔI_i up to a time t_n:

$$X_{vc} = X_{vc}^\infty \left\{w_1\left(1 - exp\left[-\sum_{k=1}^{n} \Delta I_{1,k}\right]\right) + (1 - w_1)\left(1 - exp\left[-\sum_{k=1}^{n} \Delta I_{2,k}\right]\right)\right\} \tag{6}$$

In this way, the integrals in Equation (2) are replaced by sums. For large time increments, a sub-incrementation scheme was applied to the computation of the integrals order to allow for an accurate approximation of the original integral equation.

For the melting model in Equation (3), is it straight forward to develop the incremental version of the model. Equation (3) can be approximated as

$$\Delta X_m = \left[k_{mb}\{exp[-k_{mb}(T_m - T_c)]\} \cdot (1 + (d - 1) exp[-k_{mb}(T_m - T_c)])^{\frac{d}{1-d}}\right]\Delta T \tag{7}$$

In this equation, T_m is the mid interval temperature. As for the crystallization model, a sub-incrementation can be utilized for large time increments for improving the accuracy of the approximation.

In order for the written subroutine UMATHT to work properly, both models have to communicate with each other in order to implement a re-melting step and a subsequent re-crystallization if the material cools down again. The pseudocode in Table 1 illustrates the functionality of the developed UMATHT. First, the crystallization and melting material properties explained in the last section are input. As a state variable, the activation time is introduced from the event series. It can be obtained from the event series with a user subroutine SDVINI. For each material point, this time is the time of activation during the process simulation. It is important for the crystallization

kinetics analysis as explained below. Finally, four state variables are initialized. The first one is a variable X_{vc} needed to track the crystallinity. The maximum crystallinity X_{max} at a certain material point is another parameter which is required to compute the right amount of reduced crystallinity during a melting phase. The weight factors $Weight1$ and $Weight2$ are needed for an accurate initial crystallization value upon re-crystallization. More details on the functionality of these state variables are provided below.

Table 1: UMATHT pseudocode

Let w_i, n_i, C_{i1}, C_{i2}, C_{i3}, $T_{add,i}$, $T_{m,i}$, T_g and $X_{vc\infty}$ material crystallization input properties.

Let k_{mb}, d and T_c material melting input properties.

Let t_{act} be the activation time of the material for crystallization, obtained from the event series data with a user subroutine SDVINI.

Let X_{vc}, X_{max}, $Weight1$ and $Weight2$ be the current crystallinity, the maximum obtained crystallinity, the relative importance of the first mechanism and the relative importance of the second mechanism, initialized as a state variables at the beginning of the increment.

Compute the time at the beginning of material activation: $t = TIME(2) - t_{act}$.

if $t \geq 0$ **and** $DTEMP \leq 0$ **then**   *(Negative temperature increment: Crystallization)*

    Compute the incremental contribution ΔI_1 and ΔI_2 according to Equation (5)

    Update the sum of integrands: $I_1 = I_1 + \Delta I_1, \quad I_2 = I_2 + \Delta I_2$.

    Compute the crystallinity X_{vc} according to Equation (6).

    Compute the weight Factors: $Weight1 = (X_{vc\infty}w_1(1 - \exp(-I_1)))/X_{vc}$,
                                  $Weight2 = 1 - Weight1$

    If $X_{vc} > X_{max}$ **then**

        Update maximum crystallinity: $X_{max} = X_{vc}$

    end if

else if $t \geq 0$ **and** $DTEMP > 0$ *(Positive temperature increment: Melting)*

    Compute ΔX_m according to Equation (7)

    Update the current crystallinity according to $X_{vc} = X_{vc} - \Delta X_m X_{max}$.

    Update the integrals I_1 and I_2 in order to track the right initial crystallization value for re-crystallization: $I_1 = -\log(1 - Weight1 \cdot X_{vc}/(X_{vc\infty} \cdot w_1))), I_2 = -\log(1 - Weight2 \cdot X_{vc}/(X_{vc\infty} \cdot w_2))$

end if

Compute and **Store** U, $DUDT$, $FLUX(1), FLUX(2), FLUX(3), DFDG(1,1), DFDG(2,2)$ and $DFDG(3,3)$ to implement orthotropic thermal material behavior.

Store X_{vc}, X_{max}, $Weight1$ and $Weight2$ as state variables.

Now, the computation steps illustrated in Table 1 are discussed in detail. First, the time of material activation t is computed by subtracting the activation time t_{act} from the total time $TIME$ (2) at the beginning of the increment. In this way, the time dependent evolution of crystallinity is able to start at the point of material activation, as it is the case at material deposition in the actual printing process. The overall material behavior is governed by the temperature increment in this UMATHT. For a negative increment, the crystallization model is activated, while for a positive temperature increment, the melting model is governing the material behavior. In both cases, the material activation time has to be larger or equal to zero, which means that the material has to be activated.

In the case of a negative temperature increment (crystallization), the incremental integrands ΔI_1 and ΔI_2 are computed according to Equation (5). Then, the sums $I_i = \sum_{k=1}^{n} \Delta I_{i,k}$; $i = 1,2$ are updated to account for the new contribution of the current increment. Based on the updated sums, the current crystallinity X_{vc} can be determined. Next, weight factors are computed to express the relative importance of each mechanism ($Weight1 + Weight2 = 1$). The weight factors are needed as additional information to track the change of the parameters I_i during melting. When Equation (2) is substituted in Equation (1) and simplified, one obtains

$$X_{vc} = X_{vc\infty}(w_1(1 - \exp(-I_1)) + w_2(1 - \exp(-I_2))) \tag{8}$$

Thus, the weight factors can be computed as $Weight1 = (X_{vc\infty}w_1(1 - \exp(-I_1)))/X_{vc}$ and $Weight2 = 1 - Weight1$. During a melting increment, the crystallinity X_{vc} is reduced. To start at the right crystallization value upon re-crystallization during a subsequent negative temperature increment, the parameters for I_1 and I_2 have to be updated as they determine X_{vc}. However, according to Equation (8), there are now two unknowns I_1 and I_2 with just one equation available. Here, the weight factors provide additional information as they track the contribution of each crystallization mechanism to the overall crystallinity. According to this contribution, the values for I_1 and I_2 can be updated. This will be described in more detail below. Finally, the maximum crystallinity X_{max} is updated if it is exceeded by the current crystallinity X_{vc}.

For a positive temperature increment, the melting model is activated. Based on Equation (7), an incremental degree of melting ΔX_m is computed. The current crystallinity can then be reduced as $X_{vc} = X_{vc} - \Delta X_m X_{max}$. In contrast to the crystallinity model, which is bound by a maximum crystallinity $X_{vc\infty}$, the melting model is defined between zero (fully solidified material) and 1 (fully molten material). Therefore, it is important to multiply ΔX_m by the current maximum obtained crystallinity X_{max} in order to relate the amount of melting to the actual accrued amount of crystallinity. In the current version, the UMATHT supports one re-melting process. Analyses have shown that this is sufficient since at most one re-melting phase takes place for a majority of print process simulations. To support the correct description of multiple re-melting and re-crystallization processes, the maximum crystallinity X_{max} would have to be overwritten once a re-melting phase is concluded in order to track the development of a new maximum crystallinity during re-crystallization. This could be readily implemented by introducing another state variable. As last step, the parameter I_1 and I_2 have to be updated based on the new, reduced crystallinity value. Now, the information of the weight factors is utilized from the last crystallization increment. Since the weight factors express the significance of the two crystallization mechanisms, Equation (8) can be rewritten as

$$X_{vc} = X_{vc\infty}(w_1(1 - \exp(-I_1)) + w_2(1 - \exp(-I_2)))$$

$$= Weight1 \cdot X_{vc} + Weight2 \cdot X_{vc}$$

Consequently, the parts of the equation can be set equal and solved to get I_1 and I_2. One obtains $I_1 = -\log(1 - Weight1 \cdot X_{vc}/(X_{vc\infty} \cdot w_1)))$ and $I_2 = -\log(1 - Weight2 \cdot X_{vc}/(X_{vc\infty} \cdot w_2))$. With the updated values for the sums I_1 and I_2, the correct initial crystallization value is provided upon re-crystallization of the material.

Finally, orthotropic heat transfer has to be implemented in order to describe the anisotropic thermal behavior of the deposited composite material. As discussed in the Introduction, most of the fibers align in the extrudate bead direction, which makes it the preferred direction for heat conduction. At the end of the UMATHT, the newly computed variables are stored as the new state variables.

4.   Results

Since the UMATHT described in the last section defines the combined material behavior for crystallization and re-melting in general, it can be applied to both local and global analyses. This will be illustrated in this section. However, before utilizing the UMATHT in various analyses, it was verified. For that, results were compared to a 2D model that was developed in COMSOL for the same crystallization kinetics model (Brenken, Favaloro, Barocio, DeNardo, & Pipes, 2016).

In order to investigate crystallization and re-melting behavior on the local bead level, a model was built in Abaqus where extruded beads were represented as rod-like parts, compare with Figure 1. For this model, the new AM modeling capabilities described in Section 1.3 were not utilized. Instead, the printing process was modeled by a step wise activation of boundary conditions and thermal contacts.

Figure 2 illustrates an example result from the transient printing process modeled with the local bead level model for a PEEK composite material. On the left in part a) of the figure, the temperature distribution is shown. The example result is taken just after the upper curved bead was activated. On the right in Figure 2b), the crystallinity distribution is illustrated. The material crystallization input data for this analysis was taken from paper of Velisaris and Seferis (Velisaris & Seferis, 1986). The melting material behavior was estimated based on experimental data obtained for fiber-reinforced PPS material. The figure shows the material transition from an amorphous, highly viscous fluid to a semi-crystalline solid as the crystallization phase transition takes place during cool down. Local re-melting of the first layer can be observed in the vicinity of the contact area between the beads in the region where the curved bead was just activated at extrusion temperature.
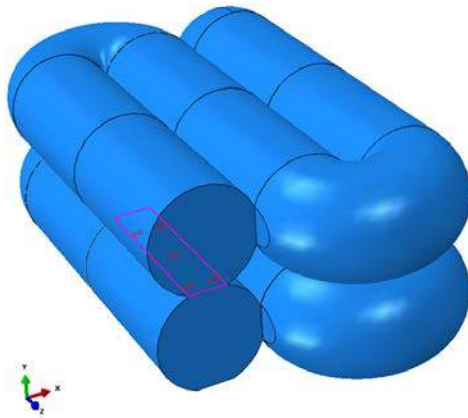
Figure 1: Local bead level model with highlighted thermal contact

a)   b)
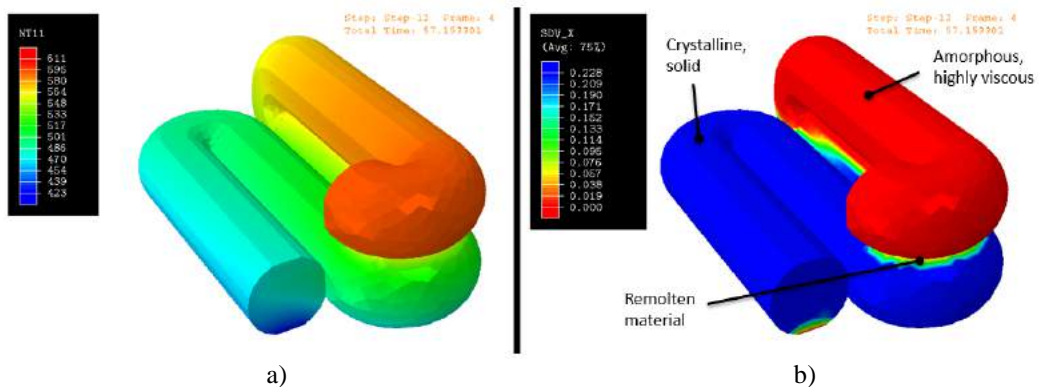
Figure 2: a) Temperature- and b) Crystallinity distribution for a time step of a transient 3D printing simulation for a PEEK composite material

Figure 3 depicts a more detailed view on the interaction of the crystallization and melting behavior of the material during a process simulation. An example output is plotted for a node on the contact area between two bead layers as illustrated in part a) of the figure. In Figure 3b), the temperature and crystallization history is shown. Before activation of the bead segment containing the node, the temperature is constant at the melting temperature. Upon activation of the material, the transient cooling process starts, based on the modeled convection and radiation heat losses. Once the temperature reaches the crystallization temperature, the material crystallizes quite rapidly up to the maximum crystallinity. As the printing simulation moves on and the bead above the node is activated, a jump in temperature can be observed. This happens due to the fact that the thermal resistance was modeled to be negligible. Since the melting model is not rate dependent, the

crystallinity is rapidly reduced as a result of the increased temperature. After that, the material cools down again and re-crystallization occurs. The illustrated example shows that the communication between the crystallization model during a negative temperature increment and the melting model during a positive temperature increment in the UMATHT works as intended and provides realistic results.

a)   b)
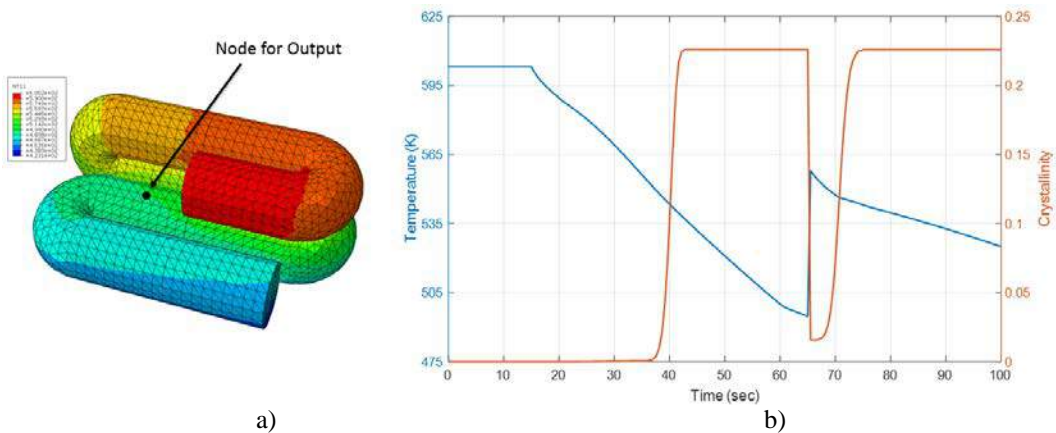
Figure 3: a) Temperature distribution with node taken for output, b) Nodal output for temperature and crystallinity for the whole analysis

In Figure 4, the final crystallinity distribution for a 50wt.% carbon fiber-reinforced PPS material is shown. In contrast to the PEEK material, the crystallization behavior of the PPS is very dependent on the cooling rate. As a consequence, the crystallinity reaches its maximum in the middle of the part where the material cools down with the slowest average cooling rate. This example stretches the importance for implementing the crystallization prediction to an ED process simulation for a semi-crystalline material. The resulting induced crystallization shrinkage for the PPS part in Figure 4 will be very different compared to the PEEK part in Figure 2, which will affect the final deformation and stress state significantly.

Finally, a crystallization result for a global part level ED printing simulation in shown in Figure 5 utilizing the CF/PPS material. Specifically, the printing process was simulated for an air inlet duct autoclave tool. In this model, voxel type elements were used and in contrast to the local level model, a single bead is just represented by a few elements. These elements were generated and then activated based on the event series as described in Section 1.3 using the new capabilities in Abaqus 2017.
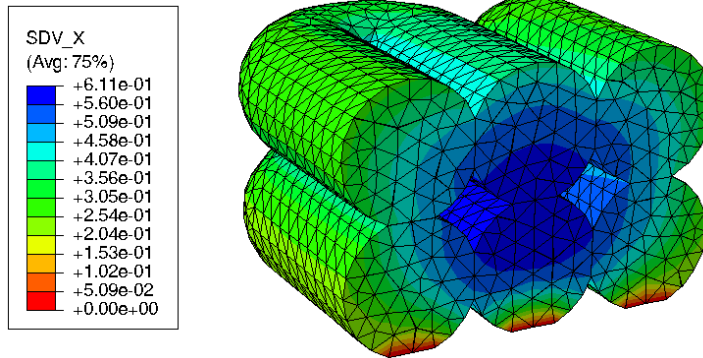
Figure 4: Crystallinity distribution of a fully crystallized part made from 50 wt.% CF/PPS after the printing process

As the deposition process is modeled, the elements begin to cool down upon activation and a crystallization front is passing from the printing bed upwards through the part. Due to slow cooling rates, maximum crystallinity is developed almost throughout the whole part. Just at the outer edges of the flange, the crystallinity is slightly lower since the material cooled too fast here. The resulting crystallization shrinkage has to be considered for subsequent deformation analyses.
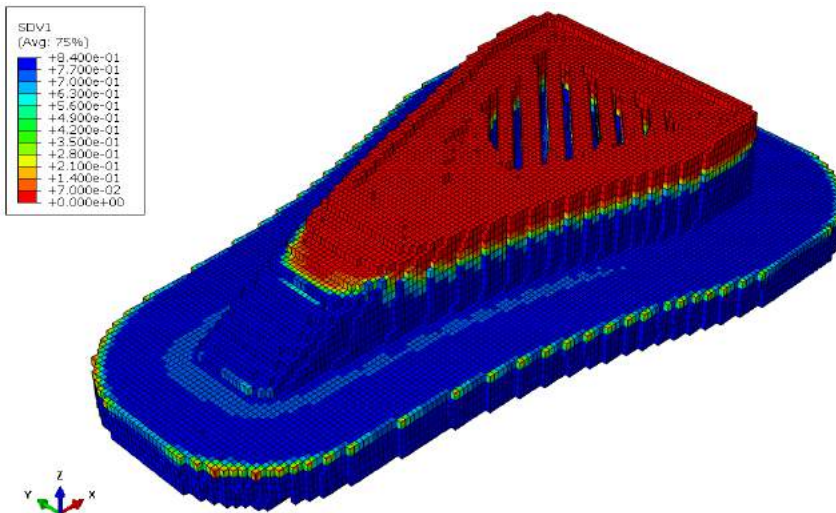
Figure 5: Crystallization distribution during the ED printing process simulation of a full scale part using 50wt.% CF/PPS

5. Conclusions and Future Work

The present work introduced a UMATHT subroutine for Abaqus that allows to simulate the crystallization and re-melting behavior for a semi-crystalline composite material during the ED process. The developed UMATHT subroutine was described in detail with a special focus on the interaction of the utilized crystallization kinetics and melting model.

Both local bead level and global part level process simulation results were shown illustrating how the crystallization and re-melting process takes place during the ED process. Results for simulated PEEK and PPS composite materials were very different indicating that the crystallization behavior is very dependent on the utilized material. As the crystallization process induces additional shrinkage to the material based on the amount of developed crystallinity in the material, the modeling and prediction of the crystallization behavior is an essential step towards modeling the overall part solidification process during ED.

Future work will incorporate the development of a UMAT to describe the viscoelastic material behavior. During cool down, the material transitions from a viscous fluid to a viscoelastic solid and stress relaxation takes place. This behavior has to be characterized and modeled for an accurate process simulation. Here, the UMATHT will provide the thermal and crystallization histories during the transient ED simulation, while the UMAT will govern the temperature and crystallization dependent mechanical properties. In addition, the crystallization shrinkage will be characterized and implemented in the full process simulation with a UEXPAN in the order to account for the effects of the additional shrinkage in a mechanical analysis.

6. References

1. Brenken, B., Favaloro, A., Barocio, E., DeNardo, N. M., & Pipes, R. B. (2016). "Development of a Model to Predict Temperature History and Crystallization Behavior of 3D Printed Parts Made From Fiber-Reinforced Thermoplastic Polymers". *SAMPE conference,* May 23-26, Long Beach, CA.
2. Chapman, T., Gillespie, J., Pipes, R., Manson, J.-A. E., & Seferis, J. (1990). "Prediction of Process_induced Residual Stresses in Thermoplastic Composites". *Composite Materials, 24*, 616-643.
3. Dassault Systémes Simulia Corp. (2017). SIMULIA User Assistance 2017, Abaqus Manual. Providence, RI.
4. DeNardo, N. M. (2016). "Additive Manufacturing of Carbon-Fiber Reinforced Thermoplastic Polymers, Master Thesis", Purdue University, West Lafayette, IN.
5. Desio, G., & Rebenfeld, L. (1992). "Crystallization of Fiber-Reinforced Poly(phenylene sulfide) Composites. II. Modeling the Crystallization Kinetics". *Applied Polymer Science, 45*, 2005-2020.
6. Favaloro, A. J., Brenken, B., Barocio, E., & Pipes, R. B. (2017). "Simulation of Polymeric Composites Additive Manufacturing using Abaqus". *Sience in the Age of Experience conference,* Dassault Systemes, May 15-18, Chicago, IL.
7. Greco, A., & Maffezzoli, A. (2003). "Statistical and Kinetic Approaches for Linear Low-Density Polyethylene Melting Modeling". *Applied Polymer Science, 89*, 289-295.

8. Heller, B., Smith, D., & Jack, D. (2016). "Computing Mechanical Properties From Orientation Tensors for Fiber Filled Polymers in Axisymmetric Flow and Planar Deposition Flow". *American Conference on Composite Materials,* September 19-22, Williamsburg, VA.

9. Love, L. J., Kunc, V., Rios, O., Duty, C. E., Elliott, A. M., Post, B. K., . . . Blue, C. A. (2014). "The importance of carbon fiber to polymer additive manufacturing". *Materials Research, 29*(17), 1893-1898.

10. Oarkridge National Laboratory. (2016). "Laboratory Directed Research & Development", Retrieved November 2016, from https://www.ornl.gov/content/laboratory-directed-research-development

11. Sawyer, K. (2016). "What Makes AMIE, the 3D printed home and vehicle, unique?" Retrieved from energy.gov: https://energy.gov/eere/articles/what-makes-amie-3d-printed-home-and-vehicle-unique

12. Thermwood. (2016). "Large Scale Additive Manufacturing". Retrieved December 2016, from http://thermwood.com/lsam/lsam_main.htm

13. Velisaris, C., & Seferis, J. (1986). "Crystallization Kinetics of Polyetheretherketone (PEEK) Matrices". *Polymer Engineering and Science, 26*(22), 1574-1580.

14. Wunderlich, B. (1976). "Macromolecular Physics. Volume 2: Crystal Nucleation, Growth, Annealing". New York, San Francisco, London: Academic Press, Inc.